CrossMark

ORIGINAL PAPER

The Calculation Method for Backfill Volume of Road Collapse in Mining Subsidence Based on GIS

Jinpeng Zhang · Limin Liu · Wei Peng

Abstract There has been a significant development in the evaluation of methods to predict ground movement due to underground extraction based on geographical information systems (GIS). In order to make the calculation of the backfill volume of road collapse more convenient, the calculating methods of backfill volumes of straight road collapse and bent road collapse due to mining subsidence are derived based on GIS in this paper. To ensure the calculation accuracy of backfill volume, the interpolation method is used for the calculation of backfill volumes of road collapse in mining subsidence. Calculation procedure: Firstly, the area of arbitrary cross-section of road is calculated by geometric method. Further, the backfill volume of road collapse between the two adjacent cross-sections is the product of the area of cross-section and the calculating step. The total backfill volume of road collapse is calculated by the sum of the backfill volume of road collapse between multiple adjacent cross-sections. Then, the calculating methods are embedded in the GIS platform for calculation. The backfill volume of the railway collapse after the 1–12# mining face is 58,113.25 m^3.

1 Introduction

The vertical and horizontal surface movements associated with coal mining are known to have considerable impacts upon natural features (Chen et al. 2016; Zahiri et al. 2006). Some serious mining subsidence can cause great loss, such as destruction of buildings and roads on the ground (Jiang et al. 2018; Yu et al. 2018). Especially in the past decade, with the large exploitation of coal resources, collapse of mined-out area occurred frequently.

Many methods have been developed for the prediction of subsidence based on empirical methods, such as those described by Hood et al. (1983). Profile functions had been effectively applied to predict subsidence above a longwall panel (Asadi et al. 2004). Semi-empirical methods of subsidence prediction based on influence functions also had been used to calculate subsidence at any surface point (Sheorey et al. 2000). In addition, numerical analyses had been used in subsidence modelling and in calculating the movement of rock strata (Zhao et al. 2004). Hao et al. (2013) used the environmental index to develop and

J. Zhang · L. Liu (✉)
College of Mining and Safety Engineering, Shandong University of Science and Technology,
Qingdao 266590, Shandong, China
e-mail: lmliuhhu@163.com

W. Peng
Shanghai Construction Engineering Research Institute Co., Ltd., Shanghai 200336, China

design an integrated evaluation model for evaluating sustainability of the ecological environment in the mining area.

Using current prediction methods can predicate vertical and horizontal components of subsidence. But, for complex, multi-seam mining area with complex mine geometry, it is difficult to use the existing methods to predicate mining induced surface subsidence (Esaki et al. 2008a, b). Due to computer-based analytical methods can realistically simulate spatially distributed time-dependent subsidence processes, the means and methods of computer technology have been adopted to predict and evaluate the surface subsidence.

The current development of geographical information systems (GIS) comprises a technology designed to support 3D modeling and conduct interactive spatial–temporal analysis (Ibrahim et al. 2012). The application of GIS in mining subsidence damage evaluation mainly includes: point object, line object and surface object. Many scholars have studied the application of GIS in the prediction and evaluation of mining subsidence, mainly including program development (Da et al. 2011; Zhang et al. 2013), model construction (Malinowska 2011), estimation method (Blachowski 2016; Malinowska and Hejmanowski 2010; Li et al. 2012) and so on. T. Esaki et al. (Esaki et al. 2008a, b) developed a new prediction method to calculate 3D subsidence by combining a stochastic model of ground movements and GIS. Lai et al. (2006) presented and verified an integrated system within a GIS environment for predicting mining subsidence coupling the time function and probabilistic integral method. Xiao et al. (2014) analyzed LS Factor under Coal Mining Subsidence Impacts in Sandy Region based on GIS. Oh et al. (2011) analyzed factors that can affect ground subsidence around abandoned mines in Jeongahm of Kangwon-do by sensitivity analysis in GIS. Suh et al. (2016) presented a case study of subsidence hazard mapping in the vicinity of an abandoned coal mine within GIS environment. A total of 85 flash flood hazard locations (n = 85) were surveyed in the field and plotted using GIS (Cao et al. 2016). Shu et al. (2013) presented a case study of subsidence hazard assessment using GIS in an abandoned coal mine area of South Korea.

The backfill in subsided area is an important method to decrease the subsidence-induced damage from coal mining. The roads affected by mining subsidence, especially for high-grade highways or railways, are often difficult to relocate or rechannel. To ensure the serviceability of roads affected by mining subsidence, the backfill method in subsided area is often adopted. (Concretely, to maintain the stability of subgrade, the method that the subgrade is backfilled when underground coal mining is often adopted.) But, it is difficult to calculate the backfill volume of the roads with different shapes and sizes, directly. So, it is necessary to establish the dynamic computational method of backfill of road collapse based on the above application of GIS in mining subsidence. In this paper, the calculating methods of backfill volume of straight road collapse and backfill volume of bent road collapse are derived. Then, the calculating methods are embedded in the GIS platform for calculation.

2 Calculation Principle of Backfill Volume of Road Collapse

Probability integral method is the most widely used method of mining subsidence prediction in numerous prediction methods. Because the movement and deformation prediction formulas contains probability integral (or its derivative), this method is called the probability integral method. The basic theory of this method is stochastic medium theory. Probability integral method is used to calculate the backfill volume of road collapse, including the backfill volume of straight road collapse and the backfill volume of bent road collapse. The calculation method is derived and then embedded in the GIS platform for calculation. The dynamic calculation of the backfill of road collapse is realized based on the GIS system.

For the calculation of backfill volume of straight road collapse: Firstly, the area of arbitrary cross-section of straight road is calculated by geometric method; Further, the backfill volume of road collapse between the two adjacent cross-sections is obtained. The backfill volume of road collapse on the road main section would be equal to the sum of the backfill volume of road collapse between multiple adjacent cross-sections. For the calculation of backfill volume of bent road collapse: The linear interpolation method is adopted in the straight line segment of bent road. The parabolic interpolation method is adopted in the bend segment of bent road. Then, the calculation

method of the area of cross-section of bent road and backfill volume is similar to that of straight road.

3 Calculation of Backfill Volume of Straight Road Collapse

3.1 Interpolation of Straight Road

Assuming that the straight road is situated in the North–South main section of subsidence trough. Figure 1 is the schematic diagram for the calculation of backfill volume of straight road collapse. In Fig. 1, the width of road is L (m), the slope angle of backfill is β (°), S_i and S_{i+1} are also the arbitrary cross-section of straight road, w_{io}, w_{iE}, w_{iF}, are also the point coordinates values of backfill boundary, w_{io} is situated in the central line of cross-section.

Assume that the starting point of road is (x_O, y_O), the calculating step is x_d, y_d, the midpoint (x_{iO}, y_{iO}) coordinates of arbitrary cross-section of straight road is:

$$\begin{cases} x_{iO} = x_O + (i-1)x_d \\ y_{iO} = y_O \end{cases} \tag{1}$$

$$\begin{cases} x_{iE} \approx x_{iA} = x_{iO} - \dfrac{L}{2} - \dfrac{W_{iO}}{tg\beta} \\ y_{iE} = y_{iO} \end{cases} \tag{2}$$

$$\begin{cases} x_{iF} \approx x_{iB} = x_{iO} + \dfrac{L}{2} + \dfrac{W_{iO}}{tg\beta} \\ y_{iF} = y_{iO} \end{cases} \tag{3}$$

It is known that the three coordinates of one cross-section are (x_{iO}, y_{iO}), (x_{iE}, y_{iE}), (x_{iF}, y_{iF}), respectively. The subsidence value.

w_{iO}, w_{iE}, w_{iF} of these three coordinates can be calculated respectively by calculation module of mining subsidence.

3.2 Calculating the Area of Cross-Section

The area of the i-th cross-section (polygon "OFCDE") is:

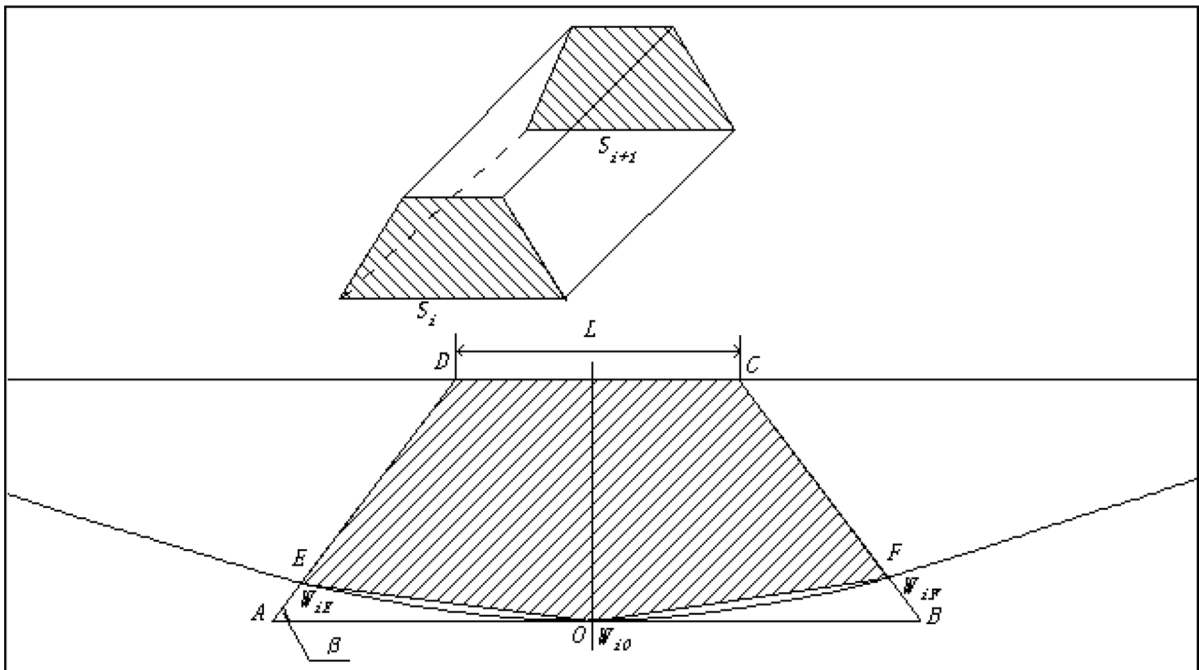$$S_i = S_{i(ABCD)} - S_{i(AOE)} - S_{i(OBF)} \tag{4}$$

where

Fig. 1 Schematic diagram for the calculation of backfill volume of straight road collapse

$$S_{i(ABCD)} = \left(L + \frac{W_{iO}}{tg\beta}\right)W_{iO} \tag{5}$$

$$S_{i(AOE)} = \frac{1}{2}\left(\frac{L}{2} + \frac{W_{iO}}{tg\beta}\right)(W_{iO} - W_{iE}) \tag{6}$$

$$S_{i(OBF)} = \frac{1}{2}\left(\frac{L}{2} + \frac{W_{iO}}{tg\beta}\right)(W_{iO} - W_{iF}) \tag{7}$$

Similarly, the area of the $(i + 1)$-th cross-section (polygon "OFCDE") is:

$$S_{i+1} = S_{i+1(ABCD)} - S_{i+1(AOE)} - S_{i+1(OBF)} \tag{8}$$

The calculation method of $S_{i+1(ABCD)}$, $S_{i+1(AOE)}$, $S_{i+1(OBF)}$ in formula (8) is the same as that of formula (5), (6) and (7).

3.3 Calculating of the Backfill Volume of Road Collapse

The backfill volume V_i of road collapse between cross-section S_i and S_{i+1} is:

$$V_i = \frac{S_i + S_{i+1}}{2}x_d$$

So, the backfill volume V_{total} of road collapse on the road main section is:

$$V_{\text{total}} = \sum_{i=1}^{n} V_i$$
$$= \left(\left(\frac{S_0 + S_n}{2}\right) + (S_1 + S_2 + \cdots + S_{n-1})\right)x_d$$

The calculating method of the backfill volume of road collapse in the East–West main section is the same as that of the backfill volume of road collapse in the North–South main section.

The smaller the calculating step x_d is, the higher the calculation accuracy is. However, over-small calculating step will extend the calculating time of computer. Obtained by multiple tests: the calculating step x_d in this range ($0 \leq x_d \leq$ L/2) has little effect on the calculation accuracy (as shown in Fig. 2).

When the road is in a skew line (that is, the straight road is situated in the non-princip of subsidence trough), (this is only a special case of bent roads), the interpolation method of the coordinate is as fellows:
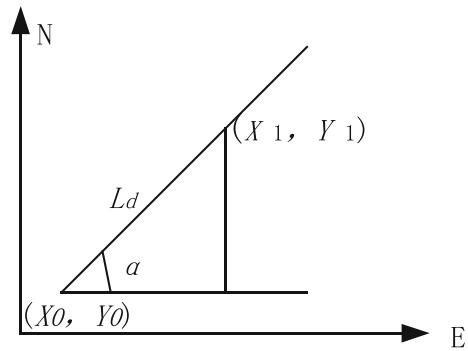
Fig. 2 Coordinate interpolation of skew line road. (x_O, y_O) is the starting point coordinate of road collapse calculation, α is the angle between the road and the East–West direction, L_d is the step of interpolation calculation

$$\begin{cases} x_i = x_0 + L_d(i - 1)\cos\alpha \\ y_i = y_0 + L_d(i - 1)\sin\alpha \end{cases} \tag{9}$$

The calculating of the backfill volume of the straight road that is situated in the non-princip of subsidence trough can reference the calculating of the backfill volume of bent road in fourth quarter.

4 Calculation of Backfill Volume of Bent Road Collapse

4.1 Interpolation Method of Bent Road

When the bent road is situated above coal face (as shown in Fig. 3), the bent road is deemed as a line object in GIS. When the road is inputted by digitization or built database by other ways, assume that any coordinate is (x_i, y_i), $i = 1,2,3\ldots n$. The distance between the two adjacent points is related to the curvature of bent road. Usually, at the gentle bend segment of bent road, the number of points is less and
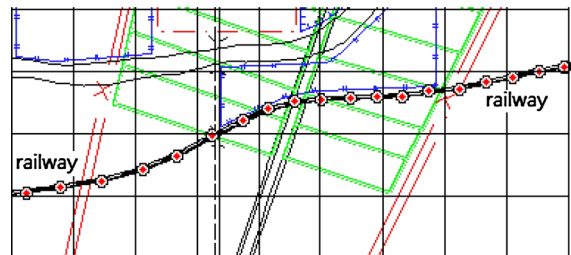
Fig. 3 Location diagram of bent road

the distance between two adjacent points is larger. At the steeply bend segment of bent road, the number of points is more and the distance between two adjacent points is smaller. In order to ensure the calculation accuracy of backfill volume of road collapse, it is necessary to increase the density of calculating point. So, the interpolation is necessary on the basis of the original digital coordinate.

The requirement of interpolation and basic hypothesis:

① The coordinate of interpolation are merely used for the mining subsidence calculation of discrete points, and the geographic information and spacial form of bent road is not changed.

② To ensure the calculation accuracy of backfill volume of road collapse, the interpolation points should be situated on the primary bent road as far as possible.

③ After interpolation, the distances between arbitrary two adjacent points are less than or equal to the prescribed step.

④ The bent road is a continuous open curve.

There may be two cases in the original digital bent road: ① The linear interpolation is adopted in the straight line segment (that is, the slopes of at least three adjacent points are equal), and the linear interpolation method is the same as the formula (9); ② The parabolic interpolation is adopted in the bend segment (that is, the slopes of at least three adjacent points are unlikeness).

1. The linear interpolation method in the straight line segment of bent road

Assume that the function value of the end point of known interval: $y_k = f(x_k), y_{k+1} = f(x_{k+1})$. The linear interpolation polynomial is required that:

$$L_1(x_k) = y_k$$

$$L_1(x_{k+1}) = y_{k+1}$$

The geometric meaning of $y = L_1(x)$ is the straight line through the two points: (x_k, y_k) and (x_{k+1}, y_{k+1}). As shown in Fig. 4a, the geometric expressions of $L_1(x)$ can be derived directly from the geometric meaning.

$$L_1(x) = \frac{x_{k+1} - x}{x_{k+1} - x_k} y_k + \frac{x - x_k}{x_{k+1} - x_k} y_{k+1} \qquad (10)$$

From the formula (10), it can be understood that $L_1(x)$ is made up of two linear functions that are $l_1(x) = \frac{x - x_{k+1}}{x_k - x_{k+1}}$ and $l_{1+1}(x) = \frac{x - x_k}{x_{k+1} - x_k}$, respectively. The coefficient of two linear functions are y_k and y_{k+1}, respectively. So, the expression of $L_1(x)$ is:

$$L_1(x) = y_k l_k(x) + y_{k+1} l_{k+1}(x) \qquad (11)$$

Obviously, $l_k(x)$ and $l_{k+1}(x)$ are also linear interpolation polynomials. At the node x_k and x_{k+1}, $l_k(x)$ and $l_{k+1}(x)$ satisfy the condition:

$$l_k(x) = 1, \quad l_k(x_{k+1}) = 0,$$

$$l_{k+1}(x_k) = 0, \quad l_{k+1}(x_{k+1}) = 1,$$

$l_k(x)$ and $l_{k+1}(x)$ are linear interpolation basic function, Fig. 4b are the images of $l_k(x)$ and $l_{k+1}(x)$.

In addition, the functions of the system should be also satisfied:

$$\sqrt{(x_k - x)^2 + (y_k - y)^2} \leq L_d \qquad (12)$$

where L_d is the minimum distance between two adjacent points.

2. The parabolic interpolation method in the bend segment of bent road

① Quadratic interpolation basic function

Assume that three nodes of interpolation are x_{k-1}, x_k, x_{k+1}, respectively. Quadratic interpolation polynomial $L_2(x)$ are required to satisfy:

$$L_2(x_j) = y_j, \quad (j = k - 1, k, k + 1), \qquad (13)$$

The basic functions $L_{k-1}(x), L_k(x), L_{k+1}(x)$ is quadratic function. And the basic functions in node of interpolation are satisfied:

$$\begin{cases} L_{k-1}(x_{k-1}) = 1 & L_{k-1}(x_j) = 0 & (j = k - 1, k) \\ L_k(x_k) = 1 & L_k(x_j) = 0 & (j = k - 1, k + 1) \\ L_{k+1}(x_{k+1}) = 1 & L_{k+1}(x_j) = 0 & (j = k - 1, k) \end{cases} \qquad (14)$$

It is easy to derive the quadratic interpolation basic function satisfied the formula (14). For example, derive the expression of $L_{k-1}(x)$: due to two zero points x_k and x_{k+1}, the expression of $L_{k-1}(x)$ is:
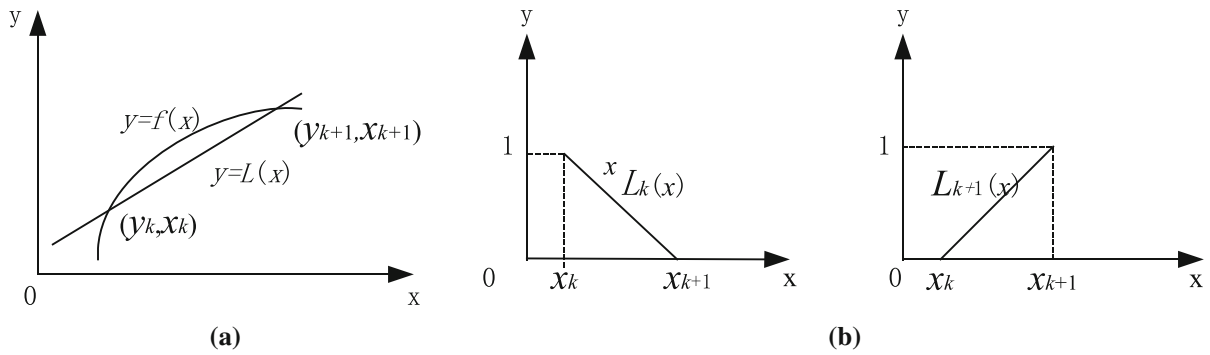
Fig. 4 Schematic diagram for the linear interpolation in the straight line segment of bent road

$$L_{k-1}(x) = A(x - x_k)(x - x_{k+1})$$

where A is undetermined coefficient. Because of the condition: $L_{k-1}(x_{k-1}) = 1$, A is defined as:

$$A = \frac{1}{(x_{k-1} - x_k)(x_{k-1} - x_{k+1})}$$

So,

$$L_{k-1}(x) = \frac{(x - x_k)(x - x_{k+1})}{(x_{k-1} - x_k)(x_{k-1} - x_{k+1})} \quad (15)$$

Similarly,

$$L_k(x) = \frac{(x - x_{k-1})(x - x_{k+1})}{(x_k - x_{k-1})(x_k - x_{k+1})} \quad (16)$$

$$L_{k+1}(x) = \frac{(x - x_{k-1})(x - x_k)}{(x_{k+1} - x_{k-1})(x_{k+1} - x_k)} \quad (17)$$

The three patterns of the quadratic interpolation basic function $L_{k-1}(x)$, $L_k(x)$, $L_{k+1}(x)$ on the interval $[x_{k-1}, x_{k+1}]$ are shown in Fig. 5.

②   Quadratic interpolation polynomial

On the basis of the quadratic interpolation basic function $L_{k-1}(x)$, $L_k(x)$, $L_{k+1}(x)$, the quadratic interpolation polynomial can be derived as follows:

$$L_2(x) = y_{k-1}L_{k-1}(x) + y_k L_k(x) + y_{k+1}L_{k+1}(x) \quad (18)$$
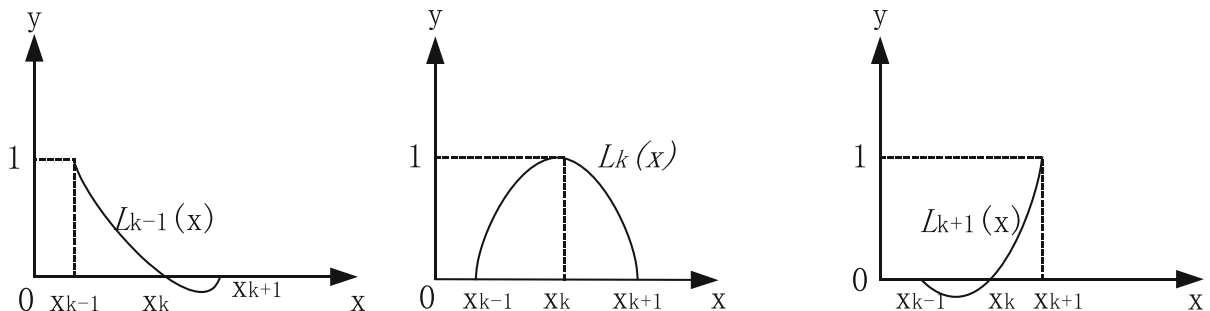
Put $L_{k-1}(x)$, $L_k(x)$, $L_{k+1}(x)$ into formula (18):

$$
\begin{aligned}
L_2(x) = \; & y_{k-1} \frac{(x - x_k)(x - x_{k+1})}{(x_{k-1} - x_k)(x_{k-1} - x_{k+1})} \\
& + y_k \frac{(x - x_{k-1})(x - x_{k+1})}{(x_k - x_{k-1})(x_k - x_{k+1})} \\
& + y_{k+1} \frac{(x - x_{k-1})(x - x_{k+1})}{(x_{k+1} - x_{k-1})(x_{k+1} - x_k)}
\end{aligned} \quad (19)
$$

In addition, the functions of the system should be also satisfied:

$$\sqrt{(x_k - x)^2 + (y_k - y)^2} \le L_d \quad (20)$$

where L_d is the minimum distance between two adjacent points.

Fig. 5 The three patterns of the quadratic interpolation basic function

4.2 Calculating w_{iO}, w_{iE}, w_{iF} of the i-th Cross-Section

The schematic diagram of the calculation of backfill volume of bent road collapse is shown in Fig. 6. The parameters in the schematic diagram are similar to those in Fig. 1: the width of road is L (m), the slope angle of backfill is β (°), and so on. From Fig. 6, it can be understood that the plane coordinate values of (x_{iO}, y_{iO}), (x_{iA}, y_{iA}), (x_{iB}, y_{iB}) in the i-th cross-section is:

$$\begin{cases} x_{iO} = x_{i0} \\ y_{iO} = y_{i0} \end{cases} \tag{20}$$

$$\begin{cases} x_{iA} \approx x_{iE} = x_{iO} - \dfrac{L}{2} - \dfrac{W_{iO}}{tg\beta} \\ y_{iA} = y_{iO} \end{cases}$$

$$\begin{cases} x_{iB} \approx x_{iF} = x_{iO} + \dfrac{L}{2} + \dfrac{W_{iO}}{tg\beta} \\ y_{iB} = y_{iO} \end{cases}$$

It is known that the three coordinates of one cross-section are (x_{iO}, y_{iO}), (x_{iA}, y_{iA}), (x_{iB}, y_{iB}), respectively. The subsidence value w_{iO}, w_{iE}, w_{iF} of these three coordinates can be calculated respectively by calculation module of mining subsidence.

4.3 Calculating the Area of Cross-Section

The area of the i-th cross-section is:

If $|w_{iB}| > |w_{iO}| > |w_{iA}|$,
$$S_{i(ABCD)} = S_{i(EFCD)} - S_{i(AOE)} + S_{i(OBF)} \tag{21}$$

If $|w_{iB}| < |w_{iO}| < |w_{iA}|$,
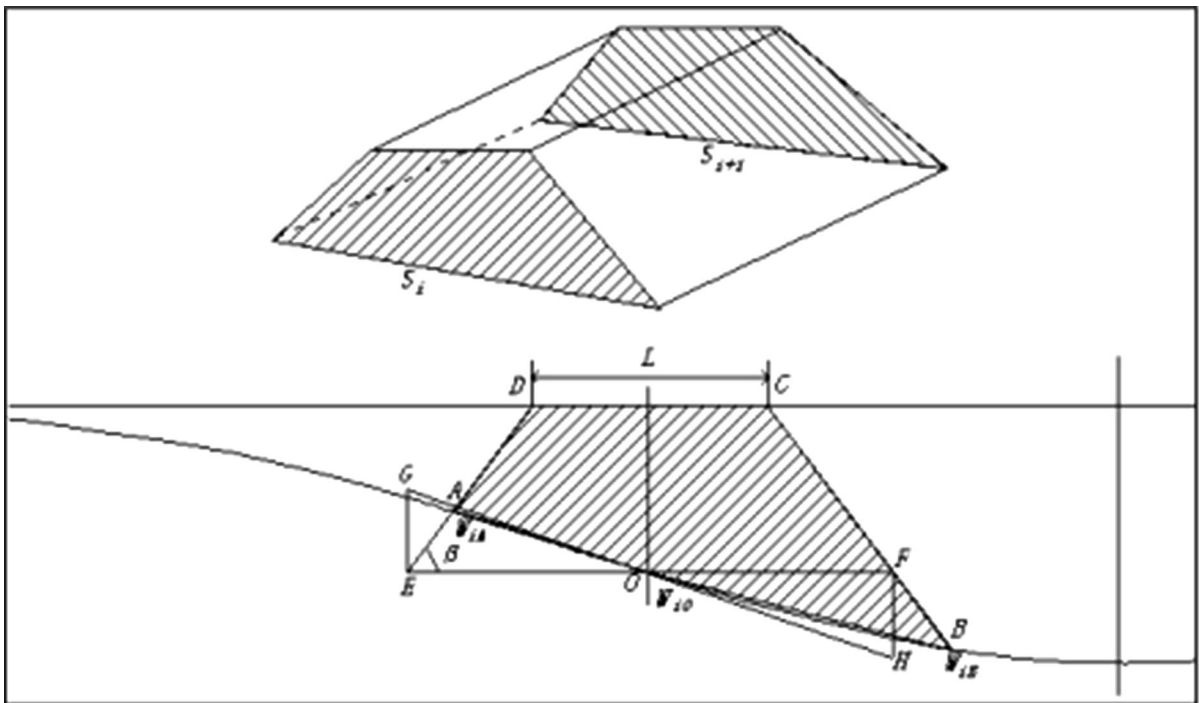$$S_{i(ABCD)} = S_{i(EFCD)} + S_{i(AOE)} - S_{i(OBF)} \tag{22}$$

where

$$S_{i(ABDC)} = \left(L + \frac{W_{iO}}{tg\beta}\right) W_{iO} \tag{23}$$

$$S_{i(AOE)} = \left| \frac{1}{2}\left(\frac{L}{2} + \frac{W_{iO}}{tg\beta}\right)(W_{iO} - W_{iA}) \right| \tag{24}$$

$$S_{i(OBF)} = \left| \frac{1}{2}\left(\frac{L}{2} + \frac{W_{iO}}{tg\beta}\right)(W_{iO} - W_{iF}) \right| \tag{25}$$

Similarly, the area $S_{i+1(ABCD)}$ of the (i + 1)-th cross-section can be calculated. The calculation procedure of $S_{i+1(ABCD)}$ is the same as that of $S_{i(ABCD)}$.

Fig. 6 Schematic diagram for the calculation of backfill volume of bent road collapse

4.4 Calculating of the Backfill Volume of Road Collapse

The backfill volume V_i of road collapse between cross-section S_i and S_{i+1} is:

$$V_i = \frac{S_i + S_{i+1}}{2} L_{di}$$

So, the backfill volume V_{total} of bent road collapse is:

$$V_{\text{total}} = \sum_{i=1}^{n} V_i$$

Based on the above researches, the author works out a program used in calculation of backfill volume of road collapse due to mining subsidence by Fortran90 language under Visual Fortran 6.5. With this program, the backfill volumes of straight road collapse and bent road collapse due to mining subsidence are calculated.

5 Example Analysis

The example region consists of 12 mining areas numbered 1#–12#. The bent railroad passes through the upper part of the mining areas. The pavement width and slope angle of the railway is 7 m and 35°, respectively. The layout of the mining face is presented in Fig. 7. The coal seam thickness is 3.7 m. The dip length of the mining face is 130 m. The maximum and minimum strike length of the mining face are 1130 m and 940 m, respectively. And the strike length of each mining area shall be determined according to the grid distance in Fig. 7. The mining depths of working face 1–12# are 320.0 m, 320.0 m, 345.3 m, 345.3 m, 368.6 m, 396.3 m, 396.3 m, 423.3 m, 423.3 m, 451.5 m, 451.5 m and 451.5 m, respectively. The prediction parameter of probability integral method is shown in Table 1. K in Table 1 is mining influence propagation coefficient.

Put the above parameter into the program and calculate. The results are as follows:

Subsidence value <=20(mm); subsidence volume = 8992.16(m3)

20″ = <subsidence value <=50(mm); subsidence volume = 25598.26(m3)

50″ = <subsidence value <=100(mm); subsidence volume = 38490.41(m3)

100″ = <subsidence value <=200(mm); subsidence volume = 69145.74(m3)

200″ = <subsidence value <=400(mm); subsidence volume = 121006.08(m3)

400″ = <subsidence value <=600(mm); subsidence volume = 105886.69(m3)

600″ = <subsidence value <=800(mm); subsidence volume = 95189.07(m3)

800″ = <subsidence value <=1000(mm); subsidence volume = 86480.33(m3)

1000″ = <subsidence value <=1200(mm); subsidence volume = 78858.73(m3)

1200″ = <subsidence value <=1400(mm); subsidence volume = 71873.45(m3)

1400″ = <subsidence value <=1600(mm); subsidence volume = 65234.26(m3)

1600″ = <subsidence value <=1800(mm); subsidence volume = 58698.47(m3)

1800″ = <subsidence value <=2000(mm); subsidence volume = 52014.22(m3)

2000″ = <subsidence value <=2200(mm); subsidence volume = 44742.26(m3)

2200″ = <subsidence value <=2400(mm); subsidence volume = 26135.88(m3)

2400″ = <subsidence value <=2400(mm); subsidence volume = 184870.7(m3)

2400″ = <subsidence value <=2600(mm); subsidence volume = 13442.76(m3)

2600″ = <subsidence value <=2600(mm); subsidence volume = 138632.88(m3)

2600″ = <subsidence value <=2800(mm); subsidence volume = 8548.67(m3)

Subsidence value > 2800(mm); subsidence volume = 3230.4(m3)

Subsidence value > 2800(mm); subsidence volume = 6937.54(m3)

The total subsidence volume of the mining face 1-6# = 1,304,008.96(m3)–calculated date(20,170,516): calculating time(15:32:03)

T001: The backfill volume of railway collapse after 1-12# mining face (m3)58,113.25
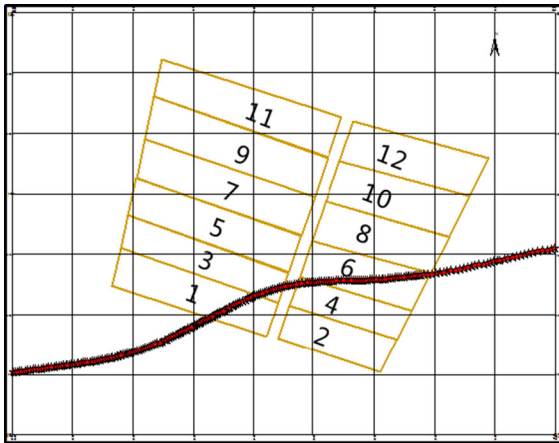
Fig. 7 Layout of the mining face

So, the backfill volume of the railway collapse after the 1–12# mining face is 58,113.25 m^3.

6 Conclusion

In order to make the calculation of the backfill volume of road collapse more convenient, the calculating methods of backfill volumes of straight road collapse and bent road collapse are derived in this paper based on the existing application of GIS in mining subsidence.

For the calculation of backfill volume of straight road collapse: Firstly, the area of arbitrary cross-section of straight road is calculated by geometric method; Further, the backfill volume of road collapse between the two adjacent cross-sections is obtained. The backfill volume of road collapse on the road main section would be equal to the sum of the backfill volume of road collapse between multiple adjacent cross-sections. The backfill volume V_{total} of road collapse on the road main section is:

$$V_{total} = \sum_{i=1}^{n} V_i = \left(\left(\frac{S_0 + S_n}{2} \right) + (S_1 + S_2 + \cdots + S_{n-1}) \right) x_d$$

For the calculation of backfill volume of bent road collapse: The linear interpolation method is adopted in the straight line segment of bent road, the parabolic interpolation method is adopted in the bend segment of bent road. Then, the calculation method of the area of cross-section of bent road and backfill volume is similar to that of straight road. The backfill volume V_{total} of bent road collapse is:

$$V_{total} = \sum_{i=1}^{n} V_i$$

Then, the calculating methods are embedded in the GIS platform for calculation. The calculations are carried out by an example. The example region consists of 12 mining areas numbered 1#–12#. The bent railroad passes through the upper part of the

Table 1 The predictive parameters of probability integral method

Mining face number	Dip angle of coal seam (°)	Subsidence coefficient	Horizontal shift coefficient	k	Downhill tgβ	Rise tgβ
1#	12	0.82	0.3	0.6	2	2
2#	12	0.82	0.3	0.6	2	2
3#	12	0.82	0.3	0.6	2	2
4#	12	0.82	0.3	0.6	2	2
5#	12	0.82	0.3	0.6	2	2
6#	12	0.82	0.3	0.6	2	2
7#	12	0.82	0.3	0.6	2	2
8#	12	0.82	0.3	0.6	2	2
9#	12	0.82	0.3	0.6	2	2
10#	12	0.82	0.3	0.6	2	2
11#	12	0.82	0.3	0.6	2	2
12#	12	0.82	0.3	0.6	2	2

mining areas. The backfill volume of the railway collapse after the 1–12# mining face is 58,113.25 m^3.

References

Asadi K, Shakhriar A, Goshtasbi K (2004) Profiling function for surface subsidence prediction in mining inclined coal seams. J Min Sci 40:142–146

Blachowski J (2016) Application of GIS spatial regression methods in assessment of land subsidence in complicated mining conditions: case study of the Walbrzych coal mine (SW Poland). Nat Hazards 84:997–1014

Cao C, Xu PH, Wang YH, Chen JP, Zheng LJ, Cencen N (2016) Flash flood hazard susceptibility mapping using frequency ratio and statistical index methods in Coalmine subsidence areas. Sustainability 8:1–18

Chen SJ, Yin DW, Cao FW, Liu Y, Ren KQ (2016) An overview of integrated surface subsidence-reducing technology in mining areas of China. Nat Hazards 81:1129–1145

Da BY, Wen XZ, Qing Y (2011) Research of mining subsided land reclamation system based on GIS. Appl Mech Mater 130–134:1858–1861

Esaki I, Djamaluddin I, Mitani Y (2008) A GIS- based prediction method to evaluate subsidence-induced damagefrom coal mining beneath a reservoir, Kyushu, Japan. In: Conference on subsidence-collapse SIP

Esaki T, Djamaluddin I, Mitani Y (2008b) A GIS-based prediction method to evaluate subsidence-induced damage from coal mining beneath a reservoir, Kyushu, Japan. Q J Eng Geol Hydrogeol 41:381–392

Hao Y, Hu Z, Nawrot JR (2013) Integrated evaluation of ecological sustainability of a mining area in the western region of China. Int J Environ Sci Dev 4:289

Hood M, Ewy RT, Riddle LR (1983) Empirical methods of subsidence prediction: a case study from Illinois. Int J Rock Mech Min Sci 20:153–170

Ibrahim D, Yasuhiro M, Hiro I (2012) GIS-based computational method for simulating the components of 3D dynamic ground subsidence during the process of undermininG. Int J Geomech 12:43

Jiang YJ, Wang YH, Yan P, Zhao ZH (2018) numerical simulation analysis of instability failure of coal pillar in mine room mining. J Shandong Univ Sci Technol (Nat Sci) 37(5):27–33

Lai X, Cai M, Ren F, Xie M, Esaki T (2006) Assessment of rock mass characteristics and the excavation disturbed zone In the Lingxin coal mine beneath the Xitian river, China. Int J Rock Mech Min Sci 43:572–581

Li XJ, Shao F, Li J, Liu X (2012) Evaluation to damage situation of coal mining subsidence land in mountainous area based on MSPS and GIS. Adv Mater Res 518–523:5692–5696

Malinowska A (2011) A fuzzy inference- based approach for building damage risk assessment on mining terrains. Eng Struct 33:163–170

Malinowska A, Hejmanowski R (2010) Building damage risk assessment on mining terrains in Poland with GIS application. Int J Rock Mech Min Sci 47:238–245

Oh HA, Choi SC, Lee S (2011) Sensitivity analysis for the GIS-based mapping of the ground subsidence hazard near abandoned underground coal mines. Environ Earth Sci 64:347–358

Sheorey PR, Singh KB, Singh SK, Loui JP (2000) Ground subsidence observations and a modified influence function method for complete subsidence prediction. Int J Rock Mech Min Sci 37:801–818

Suh J, Choi Y, Park HD, Yoon SH, Go WR (2013) Subsidence hazard assessment at the Samcheok Coalfield, South Korea: a case study using GIS. Environ Eng Geosci 19:69–83

Suh JW, Choi Y, Park HD (2016) GIS-based evaluation of mining-induced subsidence susceptibility considering 3D multiple mine drifts and estimated mined panels. Environ Earth Sci 75:1

Xiao W, Zhang HY, Zhang JY (2014) GIS-based analysis of LS factor under coal mining subsidence impacts in Sandy Region. J Eng Sci Technol Rev 7:73–78

Yu QG, Zhang HX, Deng WN, Zou YP (2018) the non-symmetric shape of surface subsidence caused by mining. J Shandong Univ Sci Technol (Nat Sci) 37(4):42–48

Zahiri H, Palamara DR, Flentje P, Brassington GM, Baafi E (2006) A GIS-based weights-of-evidence model for mapping cliff instabilities associated with mine subsidence. Environ Geol 51:377–386

Zhang MW, Lv WC, Yao GH (2013) The information acquisition system of subsidence mining-induced based on mobile GIS. In: Proceedings of the eighth international conference on bio-inspired computing: theories and applications (BIC-TA), pp 1165–1173

Zhao DS, Xu T and Tang CA (2004) Numerical simulation of bed separation of overburden strata induced by mining excavation. In: ISRM international symposium/3rd asian rock mechanics symposium (ARMS), pp 475–478